

Pentamethylcyclopentadienyl Transition-Metal Complexes.¹
 Electrochemistry of Transition-Metal π -Complexes. 7.²
 Cyclopentadienyl(arene)cobalt Cations: Preparation,
 Electrochemical Reduction, and Spectroscopic
 Investigation of the Paramagnetic d⁷ Monocations

U. Koelle,^{*3a} B. Fuss,^{3a} M. V. Rajasekharan,^{3b} B. L. Ramakrishna,^{*3a} J. H. Ammeter,^{3b}
 and M. C. Böhm^{3c}

Contribution from the Institute of Inorganic Chemistry, Technical University of Aachen, D-5100 Aachen, West Germany, the Institute of Inorganic Chemistry, University of Zürich, CH-8057 Zürich, Switzerland, and the Institute of Organic Chemistry, University of Heidelberg, D-6900 Heidelberg, West Germany. Received May 18, 1983

Abstract: A novel halogen/arene exchange reaction starting from $[\text{Co}(\text{pmcp})\text{X}_2]_2$ (pmcp = η^5 -1,2,3,4,5-pentamethylcyclopentadienyl, X = Cl, Br) makes accessible the $\text{Co}(\text{pmcp})(\text{arene})^{2+}$ dications. A series of these sandwich cations substituted to a varying degree by methyl groups in either ligand ring was prepared. Electrochemical (cyclic voltammetry and polarography at the DME) reduction of $\text{Co}(\text{cp})(\text{arene})^{2+}$ and $\text{Co}(\text{pmcp})(\text{arene})^{2+}$ (cp = η^5 -cyclopentadienyl, pmcp = η^5 -pentamethylcyclopentadienyl; arene = bz = η^6 -benzene, mes = η^6 -mesitylene, pmbz = η^6 -pentamethylbenzene, and hmbz = η^6 -hexamethylbenzene) salts (BF_4^- , PF_6^-) in propylene carbonate revealed two reversible one-electron reduction steps of nearly constant separation for each compound (+0.4 to -0.12 V and -0.56 to -1.1 V vs. SCE, respectively). These results are compared to the reduction potentials determined for the two-step reduction of $\text{Co}(\text{hmbz})_2^{2+}$ in the same solvent and to potentials for related sandwich systems in the literature. A regular displacement of both reduction potentials with the number and the position of the methyl substituents at either ring on comparison with the results of an INDO-SCF calculation yields a relation between the electrochemical substituent effect and the bonding of the ligand. Electrochemical and chemical ($\text{S}_2\text{O}_4^{2-}$, $\text{Co}(\text{cp})_2$) reduction yielded some of the sandwich complexes as the monocations, constituting a novel series of d⁷ sandwich systems. Solution shifts from ¹H NMR spectra of the monocations show a pronounced downfield shift of the methyl and a large upfield shift of the ring protons in line with established spin delocalization mechanisms. Low-temperature (4 K) EPR spectra of $\text{Co}(\text{hmbz})_2^{2+}$ and $\text{Co}(\text{pmcp})(\text{hmbz})^+$ in matrices and frozen solution show orthorhombic distortions much larger than what has been observed hitherto in comparable systems. There is evidence for a considerable degree of covalent bonding in these molecules, similar to the situation in cobaltocene.

Electron-excess sandwich complexes have evoked continuous interest by virtue of their synthetic potential as reducing agents⁴ or substrates for oxidative addition reactions.^{5,6} A point of fundamental theoretical importance is the effect of the electron(s) occupying the antibonding orbital(s) on metal-ring bonding as studied by X-ray or electron diffraction⁷ and by EPR. The latter method, applied to axially symmetric 19-electron (d⁷) sandwich molecules, can give a host of information on static and dynamic distortions and on the electronic structure of the complex.⁸

Among the limited number of group 8B organometallic complexes which have valence electrons in excess of the inert-gas configuration, the best known and most frequently studied examples are the electron-rich metallocenes $\text{Co}(\text{cp})_2$ and $\text{Ni}(\text{cp})_2^{0/+}$ (cp = η^5 -C₅H₅), the bis(arene) sandwich complexes $\text{Fe}(\text{C}_6\text{R}_6)_2^{+/0}$

(1) Part 6: (a) Koelle, U.; Fuss, B. *Chem. Ber.* **1984**, *117*, 743-752. (b) *Ibid.* **1984**, *117*, 753-762.

(2) Part 6: Koelle, U.; Salzer, A. *J. Organomet. Chem.* **1983**, *243*, C27-C30.

(3) (a) Technical University Aachen. (b) University of Zürich. (c) University of Heidelberg.

(4) (a) Astruc, D.; Hamon, J.-R.; Althoff, G.; Román, E.; Batail, P.; Michaud, P.; Mariot, J.-P.; Varret, F.; Cozak, D. *J. Am. Chem. Soc.* **1979**, *101*, 5445-5447. (b) Hamon, J.-R.; Astruc, D.; Michaud, P. *Ibid.* **1981**, *103*, 758-766.

(5) (a) Herberich, G. E.; Bauer, E. *J. Organomet. Chem.* **1969**, *16*, 301-307. (b) Herberich, G. E.; Schwarzer, J. *Angew. Chem., Int. Ed. Engl.* **1969**, *8*, 143. (c) Herberich, G. E.; Bauer, E.; Schwarzer, J. *J. Organomet. Chem.* **1969**, *17*, 445-452. (d) Herberich, G. E.; Greiss, G.; Heil, H. F. *Ibid.* **1970**, *22*, 723-730. (e) Herberich, G. E.; Schwarzer, J. *Chem. Ber.* **1970**, *103*, 2016-2023.

(6) Nesmeyanov, A. N.; Vol'kenau, N. A.; Petrakova, V. A. *J. Organomet. Chem.* **1977**, *136*, 363-370.

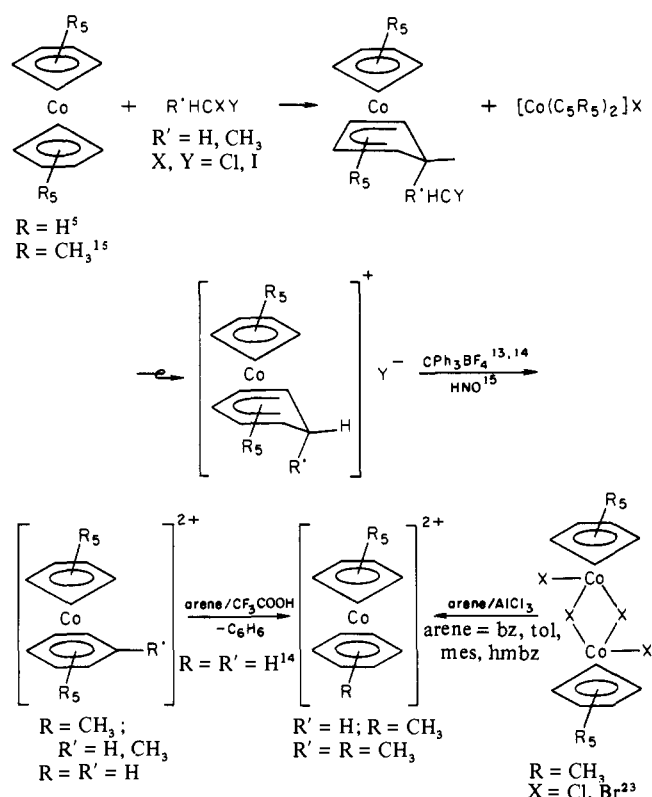
(7) Haaland, A. *Acc. Chem. Res.* **1979**, *12*, 415-422.

(8) (a) Ammeter, J. H. *J. Magn. Reson.* **1978**, *30*, 299-325. (b) Ammeter, J. H.; Zoller, L.; Bachmann, J.; Baltzer, P.; Gamp, E.; Bucher, R.; Deiss, E. *Helv. Chim. Acta* **1981**, *64*, 1063-1082 and references therein.

(9) (a) Fischer, E. O.; Röhrscheidt, F. Z. *Naturforsch., B* **1962**, *B17*, 483.

(b) Fischer, E. O.; Piesberger, U. *Ibid.* **1956**, *B11*, 758-759.

Scheme I



and $\text{Co}(\text{hmbz})_2^{2+/+}$ (hmbz = η^6 -hexamethylbenzene)¹⁰ (1), and the mixed cp/arene sandwich system $\text{Fe}(\text{C}_5\text{R}_5)(\text{C}_6\text{R}'_6)$ (R, R' =

Table I. ^1H NMR Spectroscopic and Analytical Data for Complexes $\text{Co}(\text{C}_5\text{R}_5)(\text{C}_6\text{R}'_6)^{2+/+}(\text{CoL}_1\text{L}_2^{2+/+})$

	L_1	L_2	^1H NMR (vs. internal Me_4Si^a)				solvent	yield, %	calcd		found	
			C_5H	C_5Me	C_6H	C_6Me			% C	% H	% C	% H
3c (PF_6) ₂	cp	hmbz	6.33			2.82	CD_3NO_2					
3d (PF_6) ₂	pmcp	bz		2.20	7.28		CD_3NO_2	75	34.18	3.76	34.08	3.70
3e (PF_6) ₂	pmcp	mes		2.05	6.73	2.60	CD_3NO_2	75	37.36	4.50	37.31	4.44
3g (PF_6) ₂	pmcp	hmbz		1.83		2.42	CD_3NO_2					
3c (PF_6) ^b	cp	hmbz	≈ -57			17.2	CD_2Cl_2					
3d (PF_6) ^b	pmcp	bz		41.3	≈ -4		CD_2Cl_2					
3e (PF_6) ^c	pmcp	mes		45.6	-17.6	10.4	CD_2Cl_2	70	49.68	5.92	49.44	5.80
3f (PF_6) ^c	pmcp	pmbz						80	51.75	6.40	51.61	6.25
3g (PF_6) ^c	pmcp	hmbz		50.3		23.8	CD_2Cl_2	85	52.70	6.63	52.51	6.69

^aChemical shifts of the paramagnetic substances are referred to internal Me_4Si in the neat solvent by selecting the appropriate reference frequency of the lock signal; see text. ^bPrepared by in situ reduction of the dication with a stoichiometric proportion of $\text{Co}(\text{cp})_2$. ^cFrom reduction of the dications with aqueous $\text{S}_2\text{O}_4^{2-}$.

H, alkyl) (**2**).^{4,11,12} A structural counterpart to the latter complexes would be the cobalt sandwich cations $\text{Co}(\text{C}_5\text{R}_5)(\text{C}_6\text{R}'_6)^{n+}$ (**3**), which are isoelectronic with **2** if $n(\mathbf{3}) = n(\mathbf{2}) + 1$.

Salts of the dication $\text{Co}(\text{cp})(\text{bz})^{2+}$ (**3a**²⁺) were prepared as early as 1961 by Fischer and co-workers¹³ but their insolubility in noncoordinating solvents and their instability in all coordinating solvents have buried them in a deep slumber until recently when Fairhurst and White¹⁴ showed that the benzene ligand in **3a**²⁺ undergoes arene exchange for higher methylated arenes in boiling trifluoroacetic acid. This reaction provides access to the complexes methylated in the benzene ring, viz., $\text{Co}(\text{cp})(\text{mes})^{2+}$ (**3b**²⁺) and $\text{Co}(\text{cp})(\text{hmbz})^{2+}$ (**3c**²⁺) ($\text{mes} = \eta^6\text{-}1,3,5\text{-trimethylbenzene}$), whose study makes part of the present work. However, as has been observed in the case of the Friedel-Crafts-catalyzed cp/arene exchange in ferrocene,⁴ a similar exchange reaction was not possible with the pentamethylcyclopentadienyl (pmcp) derivatives.¹⁴

Adapting the synthetic procedure by which cobaltocene is transformed into **3a**²⁺ (Scheme I) to decamethylcobaltocene, we recently achieved a synthesis for the pmcp derivatives $\text{Co}(\text{pmcp})(\text{pmbz})^{2+}$ (**3f**²⁺) ($\text{pmbz} = \eta^6\text{-pentamethylbenzene}$) and $\text{Co}(\text{pmcp})(\text{hmbz})^{2+}$ (**3g**²⁺).¹⁵ A less demanding and more general procedure for the preparation of $\text{Co}(\text{pmcp})(\text{arene})$ dications is outlined below.

With the exception of $\text{Co}(\text{cp})(\text{hmbz})$ (**3c**),¹⁶ which was obtained from $\text{Co}(\text{cp})(\text{C}_2\text{H}_4)_2$ and 2-butyne and was shown to possess a sandwich structure with the two rings parallel,¹⁶ only dications **3**²⁺ were reported. As a probe into unknown valencies and novel electron configurations of a known molecular structure, electrochemical oxidation/reduction starting from a stable inert-gas configuration is a particularly effective method. In order to assess the existence and stability of the lower valencies of complexes **3**ⁿ⁺ ($n = 1, 0$), we studied the electrochemical reduction of the above series of complexes by cyclic voltammetry, polarography at the DME, and small-sample electrolysis. The electroanalytical results opened the way toward the isolation of the novel 19-electron complexes **3**⁺, which in some instances could be characterized spectroscopically.

The reduction potentials found for the series **3** are compared to those of related systems such as the isoelectronic **2** and $\text{Co}(\text{hmbz})_2^{2+}$ (**1**), whose electrochemical reduction is studied for the first time, too.

Syntheses. The bis(hexafluorophosphate) **1**(PF_6)₂ was prepared according to the literature¹⁰ and its purity assessed from its

electroanalytical behavior. Complexes **3** were prepared by three different routes: the unsubstituted parent complex $\text{Co}(\text{cp})(\text{bz})^{2+}$ (**3a**²⁺) was obtained in 80% overall yield from cobaltocene by the oxidative addition/ring expansion sequence (1) originally developed by Herberich et al.⁵ Starting from decamethylcobaltocene¹⁷ a similar sequence leads to $\text{Co}(\text{pmcp})(\text{pmbz})^{2+}$ (**3f**²⁺) and $\text{Co}(\text{pmcp})(\text{hmbz})^{2+}$ (**3g**²⁺) when CH_2ClI or CH_3CHClI were the added electrophiles.¹⁵

From **3a**(BF_4)₂ the mesitylene and hexamethylbenzene derivatives $\text{Co}(\text{cp})(\text{mes})^{2+}$ (**3b**²⁺) and $\text{Co}(\text{cp})(\text{hmbz})^{2+}$ (**3c**²⁺) were prepared according to ref 14 by arene exchange in trifluoroacetic acid.

The ready availability of the (pentamethylcyclopentadienyl)cobalt(III) halides $[\text{Co}(\text{pmcp})\text{X}_2]_2$ ($\text{X} = \text{Cl}, \text{Br}$)^{1,23} prompted us to investigate the possibility of a halogen/arene exchange in these complexes. It was found that AlCl_3 catalyzes halogen/arene displacement at room temperature if the incoming arene is benzene or toluene and at slightly elevated temperature if mesitylene (40 °C) or hexamethylbenzene (80 °C) is used. Moreover, the precursor complexes to the cobalt(III) halides, the cyclopentadienylcobalt(II) halides $[\text{Co}(\text{pmcp})\text{X}]_2$ ($\text{X} = \text{Cl}, \text{Br}$),²³ can be directly treated with AlCl_3 /arene to yield $\text{Co}(\text{pmcp})(\text{arene})^{2+}$ salts. The latter reactions were used to synthesize $\text{Co}(\text{pmcp})(\text{bz})^{2+}$ (**3d**²⁺), $\text{Co}(\text{pmcp})(\text{mes})^{2+}$ (**3e**²⁺), and alternatively **3g**²⁺. Note that the reaction conditions for the introduction of methylated arene ligands are mild enough to avoid AlCl_3 -induced demethylation at the arene ring.

Chemical reduction of **3e**²⁺, **3f**²⁺, and **3g**²⁺ to the respective monocations was accomplished either by aqueous dithionite in acetate-buffered solution or by treating the suspensions of the bis(hexafluorophosphates) in methylene chloride with 1 equiv of cobaltocene at ambient temperature. From the resulting salt mixture $\text{Co}(\text{cp})_2\text{PF}_6$ was separated by fractional crystallization from methylene chloride/toluene, where it is much less soluble than the monocation salts **3PF**₆. These were obtained as intensely wine red crystalline solids.

Experimental Section

All hexafluorophosphate salts gave satisfactory analyses (C, H). For yields and spectroscopic data, see Table I.

Pentamethylcyclopentadienyl(benzene)cobalt(III) Bis(hexafluorophosphate) (3d(PF₆)₂). A total of 170 mg (0.65 mmol) of $\text{Co}(\text{pmcp})\text{Cl}_2^{1,23}$ was stirred with 1.5 g of AlCl_3 in 10 mL of benzene at 35 °C for

(10) (a) Fischer, E. O.; Lindner, H. H. *J. Organomet. Chem.* **1964**, *2*, 307-317. (b) Fischer, E. O.; Lindner, H. H. *Ibid.* **1964**, *3*, 222-229.

(11) (a) Nesmeyanov, A. N.; Vol'kenau, N. A.; Shilovtseva, L. S.; Petrakova, V. A. *J. Organomet. Chem.* **1973**, *61*, 329-335. (b) Nesmeyanov, A. N.; Solodovnikov, S. P.; Vol'kenau, N. A.; Kotova, L. S.; Sinitsyna, N. A. *Ibid.* **1978**, *148*, C5-C8.

(12) For a review, see: Silverthorn, W. E. *Adv. Organomet. Chem.* **1975**, *13*, 48-137.

(13) Fischer, E. O.; Fischer, R. D. *Z. Naturforsch., B* **1961**, *B16*, 556-557.

(14) Fairhurst, G.; White, C. *J. Chem. Soc. D* **1979**, 1531-1538.

(15) Koelle, U.; Khouzami, F. *Chem. Ber.* **1981**, *114*, 2929-2937.

(16) Jonas, K.; Deffense, E.; Habermann, D. *Angew. Chem., Int. Ed. Engl.* **1983**, *22*, 716.

(17) (a) Koelle, U.; Khouzami, F. *Angew. Chem., Int. Ed. Engl.* **1980**, *19*, 640-641. (b) Robbins, J. L.; Edelstein, N.; Spencer, B.; Smart, J. C. *J. Am. Chem. Soc.* **1982**, *104*, 1882-1893.

(18) (a) Koelle, U. *J. Organomet. Chem.* **1978**, *152*, 225-228. (b) Koelle, U. *Ibid.* **1978**, *157*, 327-334.

(19) Rajasekharan, M. V.; Giezyński, S.; Ammeter, J. H.; Oswald, N.; Hamon, J.-R.; Astruc, D. *J. Am. Chem. Soc.* **1982**, *104*, 2400-2407.

(20) Lueken, H.; Rohne, W., *Z. Anorg. Allg. Chem.* **1975**, *418*, 103-108.

(21) Lai, Yee-Hing; Tam, W.; Vollhardt, K. P. C. *J. Organomet. Chem.* **1981**, *216*, 97-103.

(22) Koelle, U. *J. Organomet. Chem.* **1980**, *184*, 379-383.

(23) Koelle, U.; Khouzami, F.; Fuss, B., *Angew. Chem., Int. Ed. Engl.* **1982**, *21*, 131; *Angew. Chem. Suppl.* **1982**, 230-240.

Table II. Electrochemical Parameters for the Reduction of Cations $[\text{CoL}_1\text{L}_2]^{2+}$ in Propylene Carbonate

			2+/+						+/0					
	L ₁	L ₂	\bar{E} , ^a V	ΔE_p , ^b mV	i^a/i^c	ν , ^d mV s ⁻¹	$E_{1/2}$, ^e V	αn ^f	\bar{E} , V	ΔE_p , mV	i^a/i^c	ν , mV s ⁻¹	$E_{1/2}$, V	αn
3a	cp	bz	+0.39 ₇	65	1.00	100	+0.41	1.2	-0.56	65	0.89	100	-0.53	1.04
3b	cp	mes	+0.310	100	1.00	50			-0.65	100	0.99	50		
3c	cp	hmbz	+0.22 ₃	75	1.2	20	+0.23	1.07	-0.77	80	1.2	20	-0.76	0.90
3d	pmcp	bz	+0.035	60	1.03	50	+0.08	0.85	-0.93	65	0.85	50	-0.90	1.1
3e	pmcp	mes	-0.035	60	1.01	50	-0.02		-1.04 ₃	70	0.94	100	-0.99 ₅	
3f	pmcp	pmbz	-0.10 ₂	75	0.98	50	-0.104	0.95	-1.09 ₂	75	1.07	50	-1.07 ₅	1.1
3g	pmcp	hmbz	-0.12	60	1.0	50	-0.11	0.85	-1.10 ₅	70	1.0	50	-1.08 ₆	1.08
1	hmbz	hmbz	+0.52 ₅	60	0.98				-1.75	170	<1, ill-defined at $\nu \leq 100$ mV/s			

^a Mean of anodic and cathodic peak potential. ^b Difference of anodic and cathodic peak potential. ^c Ratio of anodic and cathodic peak current at ν . ^d Scan rate. ^e Polarographic half-wave potential. ^f Apparent electronicity n from log plot of the polarographic wave.

10 min, the solution was hydrolyzed with water at 0 °C, the aqueous portion was separated and filtered, and the product was precipitated by addition of NH_4PF_6 . The precipitate was collected, washed with 10 mL of methylene chloride to remove traces of $\text{Co}(\text{pmcp})_2\text{PF}_6$, dissolved in dry acetone, and reprecipitated immediately by addition of ether to yield, after drying, a yellow powder.

Pentamethylcyclopentadienyl(mesitylene)cobalt(III) Bis(hexafluorophosphate) ($3e(\text{PF}_6)_2$) was prepared analogously by substituting mesitylene for benzene.

Pentamethylcyclopentadienyl(pentamethylbenzene)cobalt(II) Hexafluorophosphate ($3f(\text{PF}_6)_2$). A total of 0.95 g (0.97 mmol) of $3f\text{Cl}_2$ ¹⁵ was treated with an excess of an aqueous solution of $\text{Na}_2\text{S}_2\text{O}_4$ and NaOOC-CH_3 . The initially dark yellow solution turns red within 10 min. It was filtered, the monocation was precipitated with NH_4PF_6 , and the precipitate was dried and then reprecipitated from methylene chloride/ether.

Pentamethylcyclopentadienyl(hexamethylbenzene)cobalt(II) Hexafluorophosphate ($3g(\text{PF}_6)_2$) was prepared analogously from $3g(\text{PF}_6)_2$.¹⁵ Absorption spectrum (CH_2Cl_2) λ_{max} (ϵ): 530 (0.530), 400 nm (1.33 mol·cm⁻²).

Cyclopentadienyl(hexamethylbenzene)cobalt(II) Hexafluorophosphate ($3c(\text{PF}_6)_2$) and Pentamethylcyclopentadienyl(benzene)cobalt(II) Hexafluorophosphate ($3d(\text{PF}_6)_2$) were generated in situ for the NMR experiments by combining the dications and $\text{Co}(\text{cp})_2$ in a 1:1 molar ratio in CD_2Cl_2 under nitrogen.

For electrochemical measurements, cyclic voltammetry at a Beckman Pt-inlay electrode of 0.25 cm² area and polarography at the DME, equipment (EG&G) as described previously¹⁸ was used. Small-sample electrolysis was performed by using a Pt-gauze working electrode separated from the counterelectrode by a frit (Metrohm EA 273). An aqueous SCE served as the reference electrode (Metrohm EA 404), which has the KCl phase separated from the solution by an asbestos frit. Potentials were calibrated against the ferrocene/ferricenium (+0.375 V) or the cobaltocene/cobalticenium (-0.972 V) couples by adding ferrocene or cobalticenium chloride, whichever was more convenient, directly to the solution containing the cobalt complexes under investigation. Propylene carbonate (Burdick & Jackson Inc.) was distilled at reduced pressure under nitrogen. The solutions were made 0.1 M in $\text{N}(\text{C}_4\text{H}_9)_4\text{PF}_6$ (TBAH) as the supporting electrolyte and 5×10^{-4} – 10^{-3} M in the electroactive substance.

¹H NMR spectra were recorded on JEOL C-60 HL (60 MHz) or Bruker WH-270 (for paramagnetic samples) instruments. Because the WH-270 FT spectrometer does not operate unlocked, the solution shifts of the paramagnetic samples were determined by setting the spectrometer's internal reference frequency which couples the pulse frequency to the internal lock at a value which locates the Me_4Si signal in a $\text{CD}_2\text{Cl}_2/\text{Me}_4\text{Si}$ sample at 0 ppm. Shifts in Table I refer to this "diamagnetic" Me_4Si and should be corrected for the Knight shift of the deuterium lock signal.

EPR spectra were recorded on a Varian X-band spectrometer equipped as described previously.¹⁹ $1(\text{PF}_6)_2$ and $3g(\text{PF}_6)_2$ were diluted into the isoconstitutional iron complexes by codissolving the respective hexafluorophosphate salts in acetone and rapidly evaporating the solvent.

The magnetic susceptibility of $3g(\text{PF}_6)_2$ was determined on a Faraday balance with a specially designed sample suspension assembly as previously described.²⁰ The sample was obtained from cobaltocene reduction of the bis(hexafluorophosphate) in dichloromethane. Crystals that separated on cooling a dichloromethane/toluene solution were selected under the microscope, ground, and sealed into a quartz ampule under argon. The susceptibility as a function of temperature showed Curie-Weiss behavior between 300 and 80 K with smooth deviation toward lower susceptibility between 80 and 3.8 K. From the Curie-Weiss plot an

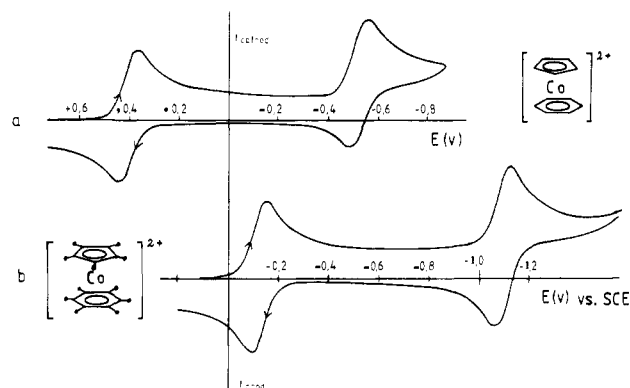


Figure 1. Cyclovoltammetric curve for (a) $\text{Co}(\text{cp})(\text{bz})(\text{PF}_6)_2$ and (b) $\text{Co}(\text{pmcp})(\text{hmbz})(\text{PF}_6)_2$ in propylene carbonate ($\nu = 50$ mV·s⁻¹).

effective magnetic moment $\mu_{\text{eff}} = 1.82 \pm 0.05 \mu_B$ and a $\theta = -26$ K are obtained.

Results

Electrochemical Reduction. The sensitivity toward nucleophiles of the lower alkylated members of the dicationic cobalt complexes 3^{2+} has largely impeded a closer investigation of their chemical properties. Nucleophilic attack generally occurs at the metal, leading to decomplexation of the six-membered ring²¹ with initial formation of solvent complexes $\text{Co}(\text{C}_5\text{R}_5)(\text{solvent})_n^{2+}$, which, for $\text{R} = \text{H}$, are isolable only if solvent is a soft donor solvent like acetonitrile.²² Thus, the pale yellow solution of $3a(\text{BF}_4)_2$ in this solvent gradually turns dark red with the appearance of a new reversible wave at +0.2 V characteristic for $\text{CoCp}(\text{NCCH}_3)_3^{2+/+}$.²² Methylation of the benzene ligand introduces enhanced stability: very slow decomplexation was observed with $3b^{2+}$ and none with $3c^{2+}$. Whereas solutions of $3a^{2+}$ and $3b^{2+}$ are stable in the less coordinating solvent propylene carbonate, $3d^{2+}$ is not. The initially yellow solution in this solvent turns light blue, persistent for days, a color that is indicative for the $\text{Co}(\text{C}_5\text{Me}_5)(\text{solvent})^{2+}$ cation.¹ Nevertheless, the electrochemical characteristics of freshly prepared solutions of $3d^{2+}$ in propylene carbonate fit the pattern exhibited by the other members of the series.

The electrochemical parameters for the reduction of the dications $1a^{2+}$ and $3a^{2+}$ through $3g^{2+}$ at the stationary Pt electrode and at the DME in propylene carbonate are collected in Table II. A representative cyclovoltammometric curve is displayed in Figure 1. It is seen that all of the cobalt complexes under investigation reduce in two discrete steps. From the peak current ratios and the apparent number of electrons exchanged, αn , extracted from the log plots of the polarographic curves, chemically reversible electron transitions are deduced even though the peak separation for the cathodic and the anodic sweep in some instances exceeds the theoretical value. The cyclic voltammograms for the isolated salts $3e(\text{PF}_6)_2$ – $3g(\text{PF}_6)_2$ were identical with those of the respective dications, which, along with the equal heights for both reduction waves (Figure 1), is a consistent proof for two mo-

Table III. EPR Parameters for Co(pmcp)(hmbz)⁺ and Co(hmbz)₂²⁺

	g_x^a	g_y	g_z	$g_e - g_z$	g_{\perp}	A_x^a	A_y	A_z	A_{\perp}	$A_y - A_x$
I Co(pmcp)(hmbz) ⁺ in Fe(pmcp)(hmbz) ⁺ /PF ₆ ⁻ , site 1	2.022	2.103	1.912	0.090	2.062	-26.0	-136.0	-56.0	-81.2	-110.0
site 2	2.003	2.084	1.858	0.144	2.043	-20.0	-141.0	-63.0	-80.5	-121.0
II Co(pmcp)(hmbz)PF ₆ in acetone, site 1	2.012	2.093	1.876	0.126	2.053	-21.5	-140.0	-58.0	-80.8	-118.5
site 2	1.986	2.067	1.850	0.152	2.027	-17.8	-142.0	-65.0	-79.9	-124.2
III Co(pmcp)(hmbz)PF ₆ in acetic anhydride	2.005	2.086	1.860	0.142	2.046	-20.0	-141.0	-62.0	-80.5	-121.0
IV Co(pmcp)(hmbz)PF ₆ in methylene chloride	2.004	2.085	1.860	0.142	2.045	-20.0	-141.0	-62.0	-80.5	-121.0
V Co(hmbz) ₂ ²⁺ in Fe(hmbz) ₂ ²⁺ /(PF ₆ ⁻) ₂ , site 1	2.023	2.128	1.858	0.144	2.076	-12.0	-137.0	-57.0	-74.5	-125.0
site 2	2.013	2.118	1.837	0.165	2.066	-9.0	-135.0	-59.0	-72.0	-126.0

^a Values evaluated by fitting to the static distortion limit $V = 1$; see text.

noelectronic reduction steps leading successively to the monocation and to the neutral sandwich.

The stability of the lower valencies of 1^{n+} and 3^{n+} ($n = 1, 0$) in propylene carbonate varies within the series. Small-sample electrolysis on the plateau of the first reduction wave was performed with complexes $3a^{2+}$, $3c^{2+}$, $3e^{2+}$, and $3g^{2+}$. Only in the case of the completely unmethylated complex $3a^{2+}$ did the monocation appear to be unstable. This was exploited further by a bulk reduction experiment in situ. Less than 1 equiv of cobaltocene was added to a suspension of $3a$ (BF₄)₂ in a CH₂Cl₂/TBAH supporting electrolyte solution, in which the dication is completely insoluble. A reddish brown solution developed rapidly, with a cyclic voltammogram indicating the formation of the monocation. After a few minutes the color faded to light brown and the peaks due to $3^{2+/+0}$ disappeared.

The methylated derivatives instead gave stable solutions of the monocations upon reduction on the first plateau which could be quantitatively reoxidized. There seemed a slight tendency to decompose for $3c^+$ over prolonged standing, apparent from decreased peak heights and the development of a new wave which can be assigned to cobaltocene.

Small-sample electrolysis on the plateau of the second reduction wave in all cases led to the development of dark solutions and precipitation of elementary cobalt along with drastically decreased cyclovoltammetric peaks. Reoxidation at a potential anodic of the first reduction did not restore the original curves; thus, the neutral sandwich molecules are obviously unstable under the experimental condition, viz., highly diluted solutions in a relatively polar solvent at ambient temperature.

The cyclovoltammetric curves for the second reduction nevertheless have the appearance of a nearly reversible electron transition with the exception of $3a^{+/0}$, $3c^{+/0}$, and $1^{+/0}$. In these cases the peak current ratio deviates from unity at sweep rates ≤ 100 mV/s, indicating that the neutral sandwich is *short-lived* on the electrochemical time scale. The second reduction $1^{+/0}$ appears at a rather negative potential and is not very well developed (Figure 2). Though the height of the cathodic peak corresponds to that of the first reduction, a current rise negative of this peak must be assigned to the formation and further reduction of fragments generated in the reduction process. The corresponding anodic peak gradually disappears at scan rates ≤ 100 mV/s. The rather large displacement of the cathodic and the anodic peak, 3 times that of the first reduction, which indicates a very slow electron transfer, is observed only at Pt. A peak separation of 70 mV was measured at the HMDE.

¹H NMR Spectra. Solution contact shifts in the monocations $3c^+ - 3g^+$ were measured in CD₂Cl₂ at ambient temperature. Signals of $3g^+$ were followed to lower temperature and were found to shift linearly with $1/T$ to lower field in the limited temperature range accessible (300–170 K). Typical line widths were 100 Hz for ring protons, 30 Hz for methyl protons at the benzene, and 60 Hz for methyl protons at the cp ring. Care has to be taken to obtain the spectrum of a single valency. If the spectrum of

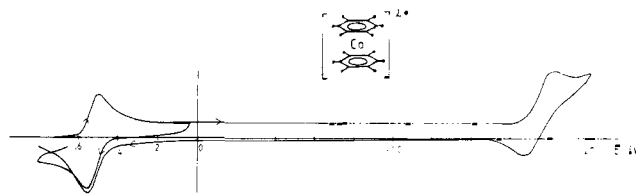


Figure 2. Cyclovoltammetric curve for Co(hmbz)₂(PF₆)₂ in propylene carbonate ($v = 100$ mV·s⁻¹).

the pure monocation (e.g., $3g^+$) was recorded in nitromethane-*d*₃, the spectral features were identical with those in dichloromethane. On addition of $\sim 1/3$ molar equiv of the dication $3g^{2+}$, lines due to the methyl groups in the paramagnetic complex were broadened and shifted toward higher field whereas lines due to the diamagnetic form were absent. This shows that the homogeneous electron exchange is fast on the NMR time scale and the spectrum is affected by the presence of the diamagnetic form. This difficulty is best circumvented by choosing a solvent/counterion combination that ensures the solubility of only the reduced form. It was found that the bis(hexafluorophosphates) of cations 3^{2+} are virtually insoluble in dichloromethane. A slightly less than stoichiometric amount of the reducing agent (cobaltocene) in the in situ reduction experiments thus did not affect the line position when dichloromethane was the solvent and hexafluorophosphate the counterion. Room-temperature shifts are given together with the positions of the diamagnetic precursor dications in Table I. The assignment was made on the basis of integrated intensities and was found to be in full agreement with shifts observed for similar methylated d⁷ sandwich systems.²⁴

EPR Spectra. EPR of sandwich compounds, with degenerate or near-degenerate electronic ground states, yields information on the bonding parameters on the one hand and the dynamic Jahn-Teller parameters on the other. The systems studied are mostly d⁵ and d⁷ sandwich complexes of the first-row transition-metal series.^{8,19,25,26} The main phenomena observed in all these complexes are the dependence of g and A tensors on the host lattice and the observation of multiple chemically inequivalent sites within a given host, caused by the changes in the relative composition of the ground electronic state wave function.

Well-resolved spectra (Figure 3) were obtained at liquid helium temperatures for Co(hmbz)₂²⁺ ($1a^{2+}$) and Co(pmcp)(hmbz)⁺ ($3g^+$) in the corresponding iron complex host lattices. The latter species was also investigated in frozen solution medium in acetone, acetic anhydride, and methylene chloride. The g and A parameters were extracted by means of computer simulation²⁷ and are shown

(24) Rettig, M. F. In "NMR of Paramagnetic Molecules"; LaMar, G. N., Horrocks, D. DeW., Jr., Holm, R. H., Eds.; Academic Press: New York, 1973; pp 220 ff.

(25) Ammeter, J. H.; Swalen, J. D. *J. Chem. Phys.* 1972, 57, 678–698.

(26) Weber, J.; Goursot, A.; Pénigault, E.; Ammeter, J. H.; Bachmann, J. *J. Am. Chem. Soc.* 1982, 104, 1491–1506.

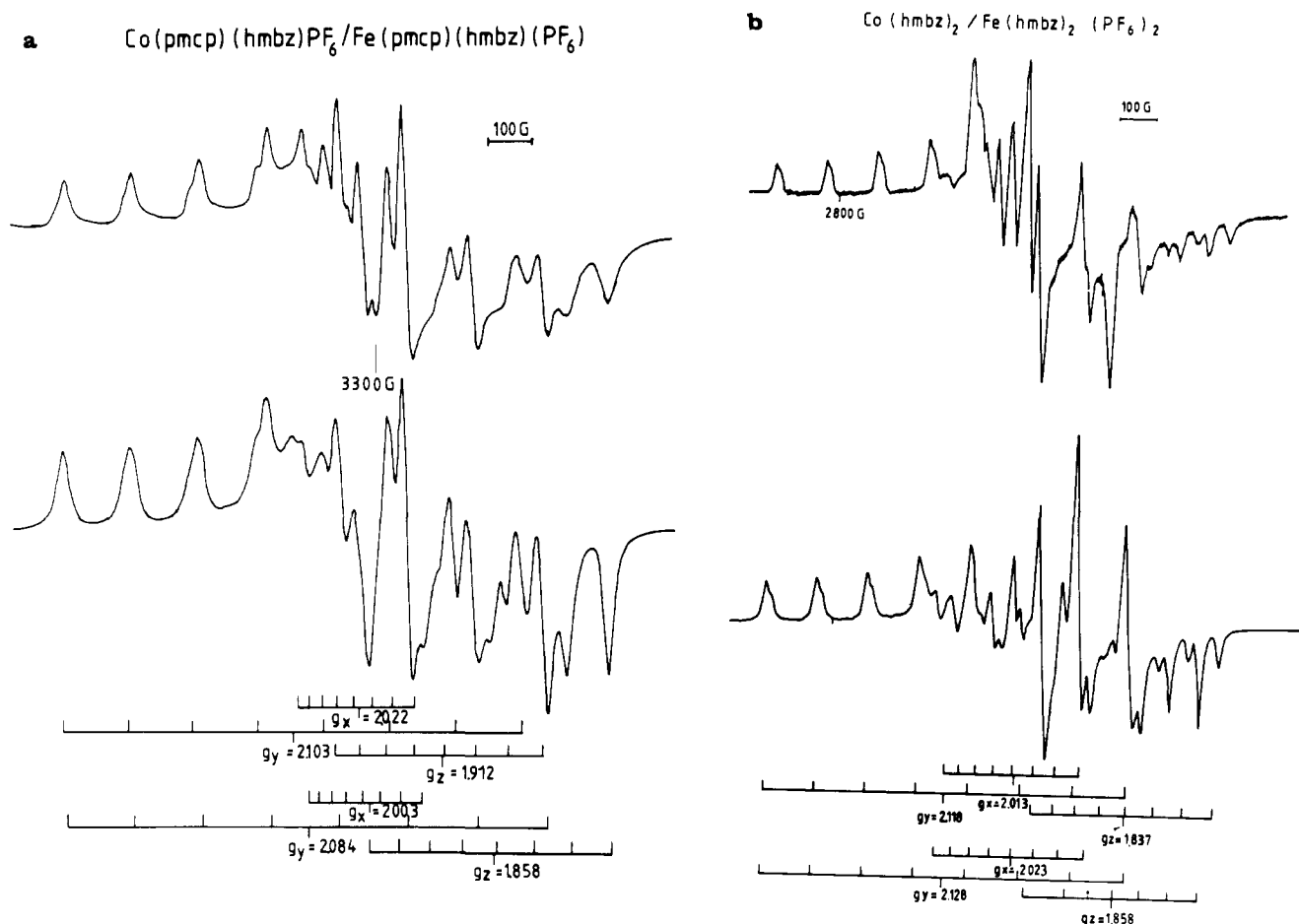


Figure 3. EPR spectra at 4 K of (a) $\text{Co}(\text{pmcp})(\text{hmbz})\text{PF}_6$ and (b) $\text{Co}(\text{hmbz})_2(\text{PF}_6)_2$ diluted to 3% in the isoconstititutional iron host lattices.

Table IV. Jahn-Teller and Covalency Parameters Derived from EPR Data (Table III) for $\text{Co}(\text{pmcp})(\text{hmbz})^+$ and $\text{Co}(\text{hmbz})_2^{2+}$

		k_{\parallel}	V	$k_{\parallel}V$	$\tan \alpha$	P	c_{π}^2	κ	x	x/x'
I,	site 1	0.82	0.99	0.81	17.5	152.0	0.600	81.3	0.0128	2.123
	site 2	0.83	0.61	0.51	6.97	158.9	0.625	79.6	0.0124	2.005
II,	site 1	0.83	0.79	0.66	9.67	161.4	0.636	76.5	0.0123	1.965
	site 2	0.83	0.46	0.38	5.02	156.7	0.617	80.6	0.0124	2.042
III		0.83	0.63	0.52	7.32	160.3	0.631	79.1	0.0124	1.982
IV		0.83	0.62	0.51	7.12	159.5	0.628	79.3	0.0124	1.992
V,	site 1	0.846	1.00	0.846	11.81	170.0	0.670	75.1	0.0161	1.725
	site 2	0.845	0.78	0.66	7.90	169.0	0.665	72.8	0.0159	1.736

Table V. Redox Potentials of Sandwich Complexes Associated with an 18/19- and a 19/20-Valence Electron Change

	$n+/(n-1)^a$	18/19		19/20		ref
		ox. state ^b	$E_{1/2}$	$E_{1/2}$	Δ	
$\text{Co}(\text{cp})_2$	+/0	3/2	-0.95	-1.88	0.93	18
$\text{Co}(\text{bor})_2^c$	+/0	3/2	+0.05	-1.1	1.15	18
$\text{Ni}(\text{cp})_2$	2+ / +	4/3	+0.9	+0.07	0.83	17a
$\text{Ni}(\text{pmcp})_2$	2+ / +	4/3	+0.3	-0.7	1.0	17a,b
$\text{Fe}(\text{hmbz})_2$	2+ / +	2/1	-0.48	-1.46	0.98	30d

^a Change in complex charge for the 18/19-transition. ^b Change in oxidation state of the central metal for the 18/19-transition. ^c bor = $\eta^5\text{-C}_5\text{H}_5\text{BC}_6\text{H}_5$

in Table III. Whenever there was more than one site the temperature variation of the spectrum was followed up to a point where the more "axial" sites vanished due to faster spin-lattice relaxation, thus leading to the observation of a single site. The spin Hamiltonian parameters obtained on simulating this simpler spectrum were carried over as a guide to fit the more complicated

lower temperature spectrum. Whereas the g_z , A_z and g_y , A_y values are accurate to within ± 0.001 for g and $\pm 1.0 \times 10^{-4} \text{ cm}^{-1}$ for A , the values for g_x and A_x are susceptible to larger errors, viz., ± 0.01 for g_x and $\pm 5 \times 10^{-4} \text{ cm}^{-1}$ for A_x . The assignment of the g components to the molecular framework, z being along the principal molecular axis, was made in analogy with other d^7 sandwich systems analyzed previously by us.^{8,19}

Application of the theory for EPR spectra of d^7 sandwich molecules^{8,19,25,26} allows the extraction of the parameters listed in Table IV, via eq 1-6 for the case of small (vibronic coupling case, eq 1a-6a) and large (static limit, eq 1b-6b, first order in ζ ($\delta \gg \zeta$)) distortion.

$$g_z = g_e - 2k_{\parallel}V \cos \alpha \quad (1a)$$

$$g_{\perp} = (g_e + 5x_2) \sin \alpha \quad (2a)$$

$$\delta g = g_y - g_x = 6(1 + V \cos \alpha)x_1 \quad (3a)$$

$$A_z = c_{\pi}^2 P \{ \frac{2}{7} - \kappa - 2V \cos \alpha - \frac{3}{7}((R_4 - R_5)3V \cos \alpha)x_1 \} \quad (4a)$$

$$A_{\perp} = c_{\pi}^2 P \{ -\frac{1}{7} - \kappa + (5R_1 + \frac{3}{14}R_6)x_2 \} \sin \alpha \quad (5a)$$

$$\delta A = A_y - A_x = c_{\pi}^2 P \{ -\frac{6}{7}(1 + V \cos \alpha) + 6((R_2 + R_3)V \cos \alpha)x_1' + \frac{3}{7}((R_7 + R_8)V \cos \alpha)x_1' \} \quad (6a)$$

(27) Daul, C.; Schläpfer, C. W.; Mohos, B.; Garup, E.; Ammeter, J. H. *Comput. Phys. Commun.* **1981**, *21*, 285.

$$g_z = g_e - k_{\parallel} \zeta / \delta \quad (1b)$$

$$g_{\perp} = g_e + 5x_2 \quad (2b)$$

$$\delta g = 6x_1 \quad (3b)$$

$$A_z = c_{\pi}^2 P \{ \frac{2}{7} - \kappa - \frac{3}{7} R_4 x_1' \} \quad (4b)$$

$$A_{\perp} = c_{\pi}^2 P \{ -\frac{1}{7} - \kappa + (5R_1 + \frac{3}{14} R_6) x_2' \} \quad (5b)$$

$$\delta A = c_{\pi}^2 P \{ -\frac{6}{7} + (6R_2 + \frac{3}{7} R_7) x_1' \} \quad (6b)$$

In the above equations, $g_e = 2.0023$ is the free electron value, k_{\parallel} is the orbital angular momentum reduction factor, V is the vibronic overlap integral, frequently called the Ham factor, P and κ are the anisotropic and isotropic hyperfine coupling parameters with P being the free ion value ($g_e \beta_o g_n \beta_n \langle r^{-3} \rangle_{3d}$) and the product $A_F = -c_{\pi}^2 P \kappa$ being the Fermi contact term. x_i and x_i' ($i = 1, 2$) are the coefficients for the mixing of the excited states of energy ΔE_i above the 2E ground state into the ground state via spin-orbit coupling, R_i ($i = 1-8$), the multiplet splitting correction factors to take into account interelectronic repulsion, are obtained with the help of ligand field assignment.^{26,44}

In the strongly distorted situation (large $\tan \alpha$, vide infra), exact evaluation of the individual values of k_{\parallel} and V is not possible. Nonetheless, the product $k_{\parallel} V$ related to $\tan \alpha$ by eq 1a is still realistic as are the values of P , c_{π}^2 , and κ .

(28) Lack of data do not yet allow the establishment of a similar rule for the displacement of the 18/19- from the 17/18-transition. However, the extremely cathodic potential for the reduction of ferrocene— -2.93 V vs. SCE in DMF (Mugnier, Y.; Moise, C.; Tirouflet, J.; Laviron, E. *J. Organomet. Chem.* **1980**, *186*, C49–C52) and the inertness of 18-electron cobalt complexes such as $\text{Co}(\text{cp})(\eta^5\text{-C}_4\text{R}_4)$ to reduction (Koelle, U., unpublished) promise a regularity here, too.

(29) Fischer, E. O.; Lindner, H. H. *J. Organomet. Chem.* **1968**, *12*, P18–P20.

(30) (a) 27–40 mV/Me for the oxidation of $\text{Cr}(\text{C}_6\text{Me}_6\text{H}_n)(\text{CO})_3$; Lloyd, M. K.; McCleverty, J. A.; Connor, J. A.; Jones, E. M. *J. Chem. Soc. D* **1973**, 1768–1770. (b) 45 mV/Me for the oxidation of $\text{Mn}(\text{C}_5\text{Me}_5\text{H}_n)(\text{CO})_2\text{PPh}_3$; Connelly, N. G.; Kitchen, M. D. *J. Chem. Soc. D* **1977**, 331–337. (c) 30 mV/Me for the oxidation of $\text{Cr}(\text{C}_6\text{Me}_6\text{H}_n)_2$; Yur'eva, L. P.; Paregudova, S. M.; Nekrasov, L. N.; Korotkov, A. P.; Zaitseva, N. N.; Zakurin, N. V.; Vasil'kov, A. Yu. *J. Organomet. Chem.* **1981**, *219*, 43–51. (d) 33 mV/Me for the difference $\text{Fe}(\text{mes})_2/\text{Fe}(\text{hmbz})_2^{2+/+}$; Braitsch, D. M.; Kumarappan, R. *J. Organomet. Chem.* **1975**, *84*, C37–C39.

(31) $E(\text{M}(\text{cp})_2) - E(\text{pmcp})_2/10$: M = Cr, 49 mV;^{17b} Fe, 53 mV;¹⁷ Co, 62 mV;¹⁷ Ni, 80 mV.¹⁷

(32) The accuracy for a potential reading from a cyclic voltammogram is ± 5 mV; the reproducibility of a measurement is ± 5 –10 mV. Thus, an error up to 10 mV, depending on the number of methyl groups incorporated, is possible for shift differences in Table VI.

(33) Polarographic $E_{1/2}$ values for the reduction of cations 2^+ in aqueous LiOH from ref 4b not incorporated into Table VI are as follows: $\text{Fe}(\text{cp})\text{bz}$, -1.62 V; $\text{Fe}(\text{cp})\text{tol}$, -1.68 V; $\text{Fe}(\text{mcp})\text{bz}$, -1.69 V. Thus, the first methyl group on benzene shifts $E_{1/2}$ by 60 mV and the first methyl group on cp by 70 mV. Similar shifts are deduced from reduction potentials of the same complexes in acetonitrile.³⁴ In the iron series the shift is thus much more attenuated when the degree of methyl substitution increases.

(34) Nesmeyanov, A. N.; Denisovich, L. I.; Gubin, S. P.; Vol'kenau, N. A.; Sirotkina, E. I.; Bolesova, I. N. *J. Organomet. Chem.* **1969**, *20*, 169–176.

(35) Vlček, A. A. *Z. Anorg. Allg. Chem.* **1960**, *304*, 109–115.

(36) INDO-SCF calculations³⁷ on a series of methyl-substituted benzenes lead to the following alkyl shifts (in eV, relative to the benzene HOMO): toluene, 0.40, *o*-xylene, 0.77, 1,2,3,5-tetramethylbenzene, 1.08, hmbz, 1.09. Comparable increments are valid for a series of the neutral methyl-substituted cyclopentadienyl radicals. Thus, similar ΔE^{18} parameters are inferred for both ligand systems.

(37) Böhm, M. C.; Gleiter, R. *Theor. Chim. Acta* **1981**, *59*, 127–151, 153–179.

(38) (a) Böhm, M. C.; Gleiter, R.; Delgado-Pena, F.; Cowan, D. O. *Inorg. Chem.* **1980**, *19*, 1081–1082. (b) Böhm, M. C.; Eckert-Maksić, M.; Gleiter, R.; Herberich, G. E.; Hessner, B. *Chem. Ber.* **1982**, *115*, 754–763.

(39) Böhm, M. C. *Ber. Bunsenges. Phys. Chem.* **1981**, *85*, 755–768. Böhm, M. C. *Theor. Chim. Acta* **1981**, *60*, 233–269.


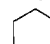
(40) Böhm, M. C. *Z. Naturforsch., A*, in press.

(41) Riley, P. E.; Davis, R. E. *J. Organomet. Chem.* **1976**, *113*, 157–166.


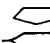
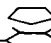
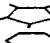
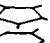
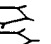
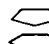
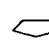
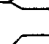
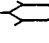

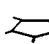

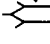
(42) (a) Clack, D. W.; Warren, K. D. *Theor. Chim. Acta* **1977**, *46*, 313. (b) Clack, D. W.; Warren, K. D. *Inorg. Chim. Acta* **1977**, *24*, 35–38. (c) Clack, D. W.; Warren, K. D. *Ibid.* **1979**, *30*, 251–258.


(43) (a) Clack, D. W.; Warren, K. D. *J. Organomet. Chem.* **1978**, *149*, 401–406; (b) **1978**, *157*, 421–429; (c) **1978**, *162*, 83–88.

(44) Clack, D. W.; Warren, K. D. *Struct. Bonding (Berlin)* **1980**, *39*, 1–41.

Table VI. Negative Shifts in Reduction Potentials of Complexes $\text{Co}(\text{C}_5\text{R}_5)(\text{C}_6\text{R}'_6)^{2+}$ in mV/CH₃ upon Methylation at the Five-Membered  and at the Six-Membered  Ring.

Upper Right Refers to $\text{M}^{2+/+}$, Lower Left to $\text{M}^{+/0}$ Reduction

					
	29 33 ^c	29 26	72 ^b 47		
	30	29		69	
	35	36	2+/+	69	18
	74		+0	23	26 2
		78		37	28
			67	29	20
					
					

^a Symbolizes e.g., $\text{Co}(\text{C}_5\text{H}_5)(\text{C}_6\text{H}_3\text{Me}_3)^{2+}$. ^b 

$[E_{1/2}(\text{Co}(\text{C}_5\text{H}_5)(\text{C}_6\text{H}_6)^{2+/+}) - E_{1/2}(\text{Co}(\text{C}_5\text{Me}_5)(\text{C}_6\text{H}_6)^{2+/+})] / 5$ mV. ^c Figures below the polygons refer to the isostructural iron complexes.

Discussion

Redox Potentials. (i) **Absolute Values.** Inspection of Table II shows that 1^{2+} is the strongest oxidant among the cobalt cations under investigation whereas the monocation 1^+ is the most resistive toward reduction, leading to a disproportionation potential for the reaction $21^+ \rightarrow 1^{2+} + 1$ of -2.27 V. These electrochemical findings illuminate the well-established chemical stability of 1^{+10} as opposed to 1^{2+} , which in solution has a strong tendency to convert to the monocation. A simple disproportionation of the dication via a 1^{3+} intermediate was discarded already by Fischer and Lindner¹⁰ for stoichiometric reasons and is further ruled out by our electrochemical observations where no further oxidation of 1^{2+} up to at least $+1.5$ V (SCE) was detectable. Most probably decomplexation of the dication is the introductory step in the formation of 1^+ from 1^{2+} in solution, where the $\text{Co}(\text{II})$ fragment serves as the reducing agent for the dication.

Reduction of the cations 3^{2+} deserves comment under a variety of aspects. Counting valence electrons, the $3^{2+/+}$ transition is isoelectronic with the reduction of the iron complex cations $2^{+/0}$. The redox potential for the latter electron transition is found to be ca. 1.7 V more negative ($E_{1/2}(\text{Fe}(\text{cp})(\text{bz}), 2a)^{+/0} = -1.42$ V in propylene carbonate; -1.62 V^{4b} in aqueous LiOH), a difference that certainly reflects the much greater oxidizing power of $\text{Co}(\text{III})$ over $\text{Fe}(\text{II})$. Noticeably the valence change $3^{+/0}$ corresponding to a 19/20-electron transition of the complex is still positive of the 18/19-transition $2^{+/0}$. From Table II it can be seen that the difference between the first and the second reduction potential within the series 3 is fairly constant (0.95–1.05 V). Table V lists redox potentials of sandwich complexes which also show electron transitions corresponding to an 18/19- and a 19/20-valence electron change, and it is seen that irrespective of the charge of the complex, the nature of the ligands and the formal oxidation state of the central metal, the difference between these two transitions is always close to 1 V. The difference between the energy required to add the 20th electron onto a 19-electron configuration and the energy needed for addition of the 19th electron, which is reflected in this potential difference, is thus similar in all of these sandwich systems.²⁸

The absolute value of the redox potential of an electron transition associated with a particular $d^{n/n+1}$ -configuration change shifts all the more positive with increasing formal oxidation state of the central metal and with neutral as opposed to anionic ligands. It is for this reason that sandwich complexes with the highest number

Table VII. Composition of the HOMOs, Net Charges, and Spin Densities of Formal Fragments of **1b**, **2a**, and **3a** according to the Semiempirical INDO Method

		fragment composition of the HOMO, %			net charges (Q) and spin densities (ρ) for the formal fragments							
		2+	1+	0	Q				ρ			
					2+	1+	0	$\Delta(2+/+)^a$	$\Delta(+/0)$	2+	1+	0
1b	Co	15	15	32	0.648	0.644	0.514	0.004	0.130	1.072	1.630	1.378
	bz	42.5	42.5	34	0.676	0.178	-0.257	0.498	0.435	-0.036	0.185	-0.189
	bz	42.5	42.5	34	0.676	0.178	-0.257	0.498	0.435	-0.036	0.185	-0.189
2a	Fe		15	26		0.378	0.375		0.003			1.231
	cp		75	50		0.180	-0.322		0.502			-0.090
	bz		10	24		0.442	-0.053		0.495			-0.141
3a	Co	6	16	14	0.632	0.661	0.682	-0.029	-0.021		1.243	1.574
	cp	54	55	66	0.592	0.049	-0.579	0.543	0.628		-0.312	0.263
	bz	40	29	20	0.776	0.290	-0.103	0.486	0.393		-0.069	0.163

^aCharge release of fragment on changing the redox state.

of valence electrons are found among the bis(arene), specifically the bis(hexamethylbenzene) complexes of Co and Ni.^{10b,29} The condition for a configuration change corresponding to two stable valencies of a sandwich to occur at a highly negative potential is that the central metal be in a low oxidation state and complexed to at least one anionic ligand. These requirements are best met by the iron complexes **2**, which by virtue of their negative redox potentials were termed "electron reservoirs" by their investigators.⁴

(ii) **Influence of Methyl Groups.** Substitution of H for Me (or other alkyl groups) at the π -ligand of a transition-metal complex induces a shift of the electron transitions to more negative values. Common examples in most cases refer to the one-electron oxidation of a species following the inert-gas rule and are of the order of 25–45 mV/Me.³⁰ Within the metallocene series, comparison of redox potentials for the +/0 transition can be made between $M(cp)_2$ and $M(pmcp)_2$ for $M = Cr, Fe, Co,$ and Ni with shifts increasing in that order from 50 to 80 mV/Me.³¹ A regular methyl shift of both redox transitions in **3** is obvious from the data in Table II. Table VI is a compilation in matrix form of the potential differences that can be extracted from the data in Table II for the first (upper right) and the second (lower left) reduction of complexes 3^{2+} , normalized to one methyl group. Note that the absolute potential values shift negative from upper left to lower right. It is seen that shifts referring to substitution at the benzene ring (enclosed in hexagons) center around 30 mV/Me whereas those referring to methylation of the cyclopentadienyl ring (enclosed in pentagons) are close to 70 mV/Me.³² Shifts tend to decrease when the absolute value lies more negative; i.e., the effect attenuates toward the fully substituted members of the series.

Similar shifts are extracted from data given in ref 4b and 33 for the iron complexes **2** and are incorporated into Table VI. As in **3**, so also in **2** methylation at cp shifts $E_{1/2}$ stronger negative than does methylation at benzene but now the whole effect is attenuated much more strongly when the number of methyl groups increases. Obviously, the potential differences are swamped if the electron transition occurs at a very negative potential.

It is intriguing to relate the shift on $E_{1/2}$ of an electron transition exerted by a substituent at the ligand of a complex to the metal–ligand interaction, and any conclusions drawn should be most elucidative if the effect of a particular substituent at different sites of the same complex is considered as in the present case.

Vlček,³⁵ on the basis of an approximate perturbation treatment, has suggested eq 7, which establishes a proportionality between

$$\Delta E^{\text{compl}} = c_{\text{lig}}^2 \Delta E^{\text{lig}} \quad (7)$$

the substituent shift in the complex, ΔE^{compl} , and the substituent shift of the free ligand, ΔE^{lig} , where the HOMO of the complex (in its reduced form) is partitioned as $\psi_{\text{compl}} = c_{\text{met}}\psi_{\text{met}} + c_{\text{lig}(1)}\psi_{\text{lig}(1)} + c_{\text{lig}(2)}\psi_{\text{lig}(2)} + \dots$. The direct application of eq 7 in most cases is impeded by the lack of data for ΔE^{lig} ³⁶ but it draws attention to the point that an implication of substituent shifts upon c_{lig} is warranted only in the case where the ΔE^{lig} are comparable.

INDO Calculations. In order to gain deeper insight into the electronic structure of **3** and the related complexes **1** and **2**, we have performed INDO calculations³⁷ on Co(bz)₂ (**1b**), on **2a**, and on **3a** in their experimentally accessible redox states. The

Table VIII. Averaged Wiberg Bond Indices (Transition-Metal to Ligand) of **1b**, **2a**, and **3a** according to the Semiempirical INDO Method

		2+	1+	0
1b	Co–bz	0.150	0.097	0.129
2a	Fe–cp		0.332	0.203
	Fe–bz		0.233	0.218
3a	Co–cp	0.304	0.164	0.114
	Co–bz	0.184	0.129	0.134

semiempirical ZDO operator has been designed to reproduce the computational results of double- ζ ab initio calculations and has been successfully applied in investigations of the photoelectron spectra and the ground-state properties in a large number of metallocene derivatives.^{38–40} The geometrical parameters for the SCF calculations were extrapolated from related metallocenes.^{7,41} We have adopted only one geometry for all valence states; nuclear rearrangements in the various cations were not considered in the present model calculations. The energy separations thus correspond to vertical differences.

The electron structure and the orbital splitting pattern of mixed sandwich complexes have been analyzed in detail by Clack and Warren,^{42–44} so we will not discuss the MO properties of our model systems explicitly. In accordance with the generally accepted bonding models for metallocenes and mixed cp/arene and bis(arene) sandwich complexes of the late transition metals,⁴⁵ the level ordering for the orbitals with significant metal-3d contribution follows the familiar sequence $d_{xz}/d_{yz}(e_1) > d_{z^2}(a_1), d_{xy}/d_{x^2-y^2}(e_2)$ in the D_n point group notation. The valence states $3a^{2+/+0}$ correspond to occupancies $e_1^{(0/1/2)}$, i.e., to a singlet, doublet, and triplet ground state. $2a^{+0}$ is associated with an $e_1^{(0/1)}$ and Co(bz)₂^{2+/+0} with an $e_1^{(1/2/3)}$ population. The INDO calculations, however, indicate the one-to-one correspondence of e_1 and $3d_{xz}/d_{yz}$ being only a rough approximation as the ligand amplitudes always exceed the 3d admixtures in the corresponding frontier orbitals (see below).

The INDO calculations predict an energy difference between $3a^+$ and $3a$ of 7.25 eV whereas $2a^+$ lies 6.29 V above **2a**. The relative difference of 0.96 eV has to be compared to the experimental difference for the $3a^{+0}$ and the $2a^{+0}$ redox transitions of 0.86 V. Likewise, the energy of the triplet **1b**⁺ is found 5.45 eV above the doublet ground state⁴⁶ of the neutral complex. The associated redox potential cannot be measured, but assuming a methyl shift of 25 mV/Me, a value of -1.45 V for the **1b**^{+/0} transition is extrapolated from the experimental value of the **1a**^{+/0} transition, which is close to $2a^{+0}$ and considerably negative of $3a^{+0}$. The remaining discrepancies between the redox potentials and the INDO–SCF energy differences in this series should be traced back to uncertainties in the extrapolated geometries. The INDO results for **1b**, **2a**, and **3a** furthermore allow a rationalization of the ligand influence (e.g., methyl shift in the redox

(45) For a compilation of quantum chemical results on transition-metal sandwich complexes, see also ref 25.

(46) The effective magnetic moment of Co(hmbz) was determined as $\mu_{\text{eff}} = 1.86 \mu_B$,^{5b} indicating a doublet ground state.

Table IX. Comparison of EPR and Jahn-Teller Parameters in d⁷ Sandwich Complexes

complex	g_{iso}	$g_z - g_e$	δg	$\tan \alpha$	$x \times 10^2$	ref
Co(cp) ₂ , Co(Rcp) ₂	1.6	0.25-0.45	0.065-0.080	0.6-2.8	0.9-1.1	25
Fe(C ₅ R ₅)(C ₆ R' ₆) (2)	1.5-1.98	0.10-0.35	0.056-0.085	0.8-8.0	0.9-1.3	19
Co(pmcip)(hmbz) ⁺ (3 ⁺)	1.97-2.01	0.09-0.15	0.081	5.0-17.5	1.2-1.3	this work
Fe(hmbz) ₂ ⁺ (4 ⁺)	1.98	0.15	0.09	5.5	1.4	19
Co(hmbz) ₂ ²⁺ (1 ²⁺)	1.99-2.003	0.144-0.165	0.105	7.9-11.8	1.6	this work

potentials) in these sandwich complexes. In Table VII the composition of the HOMOs, the net charge for the fragments, as well as the spin densities are summarized; Wiberg bond indices⁴⁷ are collected in Table VIII.

The composition of the HOMO (e_1 descendants) in the open-shell species differs from the metal-d localization properties encountered in closed-shell d⁶ sandwich complexes where the 3d amplitudes in the e_2 and a_1 MO set often exceed 80-90%. The INDO results of Table VII show a preponderance at the ligand amplitudes in comparison to the metal ($3d_{xz}$, d_{yz}) admixtures. Additionally, it is seen that the cp contributions in the mixed-ligand complexes exceed the bz character. The ratio of cp/bz character in the HOMO, normalized to one hapto position, is 55:5/29:6 = 2.68 for 3a⁺ and 3.96 for 3a (Table VII). These values should be compared with a normalized methyl shift ratio E^{cp}/E^{bz} of 2.35 for 3a^{2+/+} and 2.62 for 3a^{+/0}, taking the increments from Table VI. Even though the numerical agreement in the first case seems fortuitous, it is evident that the relative ligand contributions to the orbitals where the valence change predominantly occurs is reflected by the substituent influence pertaining to these ligands. Deviations between theory and experiment of course have their origin in electronic reorganization processes that accompany the various redox transitions. The same arguments which are presented for 3 are valid for the iron complexes 2 where an enhanced metal contribution in the HOMO is responsible for a smaller substituent influence.

The charge distributions in the ligand fragments and at the 3d centers in the different valence states of 1, 2, and 3 give some insight into the electronic redistribution encountered in the various cationic hole states. Thus, it is seen that the positive net charge at the metal is nearly independent from the overall charge of the molecule, which means that the release of electrons at the metal on oxidation is nearly fully compensated by an enhanced ligand-to-metal charge transfer. The results collected in Table VII further indicate that the cp ring is of greater importance as a donor in this process. Similar effects were evidenced in calculations on cobaltocene and ferrocene.⁴⁸ In each case the loss of electron density at the metal center is considerably smaller than would be expected on the basis of the MO composition, an effect that must be attributed to orbital reorganization during the ionization process.

A preference of cp over benzene coupling to the metal in the cationic states of 2 and 3 is also obvious from the metal-ligand and intraligand Wiberg bond indices summarized in Table VIII. The difference is most important in the dication 3a²⁺. In accord with the larger cp character in the antibonding e_1 linear combination, the metal-cp interaction is more strongly influenced when the e_1 HOMO becomes populated in the lower valencies. This result is in line with experimental observations that nucleophilic attack on 3²⁺ preferentially leads to the decomplexation of the benzene ring (vide supra).

Whether the stronger binding of benzene over cp in the neutral complexes 2 and 3 indicated by the Wiberg bond indices is of chemical significance remains open to question. The decomposition of neutral 2a in polar solvents frequently leads to ferrocene¹¹ whereas no cobaltocene could be detected in the decomposition products of neutral 3 generated by electrolysis on the plateau of

the second reduction. Release of the cp ligand in any case would lead to complete breakdown of the π complex as no benzene iron or cobalt half-sandwich complexes are known.

In summary, the INDO results allow a straightforward explanation of the larger methyl shifts in the cp ring. The nature of the covalent metal-ligand interaction depends critically on the occupation pattern of the high-lying e_1 descendants. The larger cp admixtures in e_1 are accompanied by stronger modifications of the coupling strength.

NMR Contact Shifts. As can be seen from Table I, there is a consistent upfield shift for protons attached to either ligand ring in 3⁺ and a downfield shift for all methyl protons. For either sort of proton the shift is more pronounced for cp with values ranging from 40 to 50 ppm as compared to benzene where the methyl protons are shifted only from 17 to 24 ppm. Moreover, there is a constant increase in methyl shift with increasing number of methyl groups. The latter effect has been observed in closely related systems such as 1,1'-dimethylcobaltocene (δ_{CH_3} 11²⁴), 1,2,3,4,5-pentamethylcobaltocene⁴⁹ (δ_{CH_3} 35), and decamethylcobaltocene^{17a} (δ_{CH_3} 40).

Anderson and Drago⁵⁰ have estimated the dipolar contribution to the contact shifts of cyclopentadienyl and arene sandwich complexes with the aid of Jesson's formulas⁵¹ and found that dipolar shifts are expected to be small, thus making a minor fraction of the observed solution shifts in all cases where these exceed a few ppm. In view of the similar geometry and the rather small deviation of g values from g_e in the cation complexes 3⁺ (see below), their arguments are fully valid for the present case. Solution shifts in 3⁺ therefore originate predominantly (>90%) from Fermi contact for methyl and ring protons. The consistent upfield shift of the ring protons and downfield shift of the methyl protons, following the arguments of Anderson and Drago, is conclusive evidence for spin polarization by a π mechanism where α spin from the singly occupied e_{1g} level is transferred onto ring and methyl hydrogens with alternate signs.

The greater solution shift at the five-membered ring again is mimicked by our INDO treatment. The spin densities (Table VII) indicate that spin polarization in the ligand frameworks is of significant importance in the open-shell species. In the doublet states it is always diagnosed that the spin polarization in the ligands is opposite to the spin direction at the 3d center.

Assuming a spin polarization mechanism, the spin density at the ligand carbon atoms should provide a basis for an estimate of the relative contact shifts of the methyl protons. In the case of 3a⁺ significantly larger spin densities at the cp ring are predicted in comparison to the polarization in the benzene ring (Table VII).

Solution contact shifts for Fe(cp)(hmbz) were given as 2.15 ppm for the methyl and -35 ppm for the cp-ring protons.^{4b} Though the latter value is in close agreement to what is to be expected on the basis of calculated spin densities, the downfield shift of the methyl protons appears unexpectedly small. A similar small solution shift of 4.3 ppm (downfield) is reported by Anderson and Drago⁵⁰ for the methyl protons in a sandwich system otherwise closely related to 3⁺, viz., Fe(hmbz)₂⁺ (4⁺). Shifts in 3⁺ therefore reflect a considerably more effective spin delocalization onto the ligands, indicating a higher degree of covalency in 3⁺ as compared to either 2 or 4⁺.

EPR Parameters. In discussing the results of the EPR measurements, we attempt to derive a picture for the systems 1a²⁺

(47) Wiberg, K. B. *Tetrahedron* 1968, 24, 1083-1096.

(48) SCF calculations on Fe(cp)₂^{+/0} give a net charge of 0.25 at the metal in the cation where the metal contribution to the HOMO is about 80% (see the discussion in ref 7). For Co(cp)₂, 0.66 and 0.88 were calculated for the charge on the cobalt atom in the cation and in the neutral complex, respectively, by MS-X- α ; 0.4 and 0.6 are cited as values estimated from X-ray absorption spectra (see ref 26).

(49) Koelle, U., unpublished.

(50) Anderson, S. E., Jr.; Drago, R. S. *J. Am. Chem. Soc.* 1970, 92, 4244-4254.

(51) Jesson, J. P. In ref 24, pp 18 f.

and $3g^{2+}$ by comparison of their EPR parameters with those of other d^7 sandwich systems previously determined and interpreted by us. Therefore, selected values for substituted cobaltocenes²⁶ Fe(cp)(bz) (**2**)¹⁹ and for Fe(hmbz)₂⁺ (**4**)¹⁹ are included in Table IX.

Notice first that in $1a^{2+}$ and $3g^+$ g_{iso} and g_z are closest to the free electron value (2.003) whereas the orthorhombic splitting $\tan \alpha$ is greater than in the other d^7 complexes, especially greater than in the average of the corresponding Fe(I) compounds. It may be argued that extensive substitution in itself tends to increase the deviation from axial symmetry but even so the effect with the cobalt cations is still greater than in peralkylated iron derivatives **2**. In the absence of structural data that could prove a static distortion, we attribute the rhombic splitting to a freezing of the dynamic Jahn–Teller motion of the ring carbon atoms of the free molecule by the host environment as has been found in all comparable cases studied thus far.^{8,19,25–27} Application of the theory outlined in ref 19 (eq 1–6) led to the parameters $\tan \alpha$ and $k_{\perp}V$ and, with the aid of the hyperfine tensor components, the bonding and covalency parameters of Table IV. Again, $\tan \alpha$ on the average exceeds the values observed for cobaltocene and the mixed iron complexes.

A parameter directly derived from the experimental g values is the coefficient x which describes the mixing of excited states into the ground-state wave function (vide supra). Again, x is greatest for the present systems with respect to cobaltocenes and iron complexes. Since it is inversely related to a mean energy separating the excited doublets from the doublet ground state through $x = k_{\perp}(\zeta/\Delta E)$, a greater x means more readily accessible excited states (smaller ΔE) or a much greater orbital reduction factor k .

We have recorded the absorption spectrum of $3gPF_6$ in dichloromethane between 28×10^3 and 17.4×10^3 cm^{-1} and found two absorptions in the visible region at 18.8×10^3 and 25×10^3 cm^{-1} (vide supra), the latter on the long wavelength slope of a strong band at shorter wavelength. The spectrum closely resembles that of 4^+ ,^{9a} with both absorptions shifted to shorter wavelength by 50 and 80 nm, respectively. Virtually no absorption is detected beyond 15×10^3 cm^{-1} . Most probably, as in 4^+ , the transitions are mainly of the $M \rightarrow L$ CT type. Hence, any d–d transitions masked by these bands must occur at higher energy than in either 4^+ or **2**, where d–d transitions possibly are hidden underneath a broad absorption between 13×10^3 and 15×10^3 cm^{-1} .^{4b} Thus, the optical data give an energy separation for $3a^+$ equal to or larger than in systems **2**.

The coefficient for metal-d contribution to the orbital of the unpaired electron, c_{π}^2 , as deduced from the hyperfine parameters means that about 60% of the overall spin density in $3g^+$ is on the cobalt, Co(hmbz)₂²⁺, on the other hand, is shown by EPR to be slightly more ionic, with c_{π}^2 deduced from spin Hamiltonian parameters as equal to 0.67. The c_{π}^2 values derived from the analysis of the spin Hamiltonian parameters for the mixed sandwich system are consistently less than those determined for either cobaltocene or the iron mixed sandwich complexes **2**, with less than 60% of the electron density on the metal. The x values, which are inversely related to the average $\sigma \rightarrow \pi$ and $\delta \rightarrow \pi$ transition energies and directly to the value of k_{\perp} (determined by the covalency of the d_{z^2} , d_{xy} , and $d_{x^2-y^2}$ orbitals), are larger in the compounds studied in this work than in the corresponding iron

sandwiches. However, larger covalency and smaller energy separation do not seem compatible.

As the accuracy of the spin Hamiltonian parameters (Table III) is critical to the significance of the covalency parameters which these provide the basis for and since g_x and A_x cannot be accurately determined from the spectral simulation, we have carried out a detailed analysis for Co(pmcp)(hmbz)PF₆ in Fe(pmcp)(hmbz)PF₆ (entry I in Table III) considering individual ΔE 's. Two values, designated x_1 and x_2 in eq 1a–6a, related to the a_1/e_1 and the e_2/e_1 energy separation, respectively, were introduced instead of a single x . Furthermore, g_x and A_x , whose uncertainty is the hurdle in an accurate determination of the bonding parameters, were allowed to vary. This procedure involves the assumption of a value for k_{\parallel} from EHMO calculations and the variation of the ratio x_1/x_2 and $\delta g = g_y - g_x$ until V equals 1 as we feel that the static limit of distortion has been reached in this system. For the less distorted site, I/1 in Table III, the ratio of x_1/x_2 comes to 1.15 and similar for the more distorted site, I/2, it is evaluated as 1.10 for $V = 0.99$. A similar procedure for $1a^{2+}$ led to a x_1/x_2 ratio of 1 if the value of V was not to exceed unity. Thus, in the symmetrical sandwich cation a single energy separation between the low-lying e_2/a_1 and the high-energy e_1 orbitals is still a valid assumption. The necessity of two individual x_i for the unsymmetrical cobalt complex in itself is evidence for larger orthorhombic distortion. The larger values of the x_i indicate larger orbital reduction factors in the cobalt as compared to the iron complexes and this is in keeping with the higher covalency as shown by the values of the c_{π}^2 .⁵²

In summary, spectroscopic and electrochemical data all tend in the same direction: large static distortion and a high degree of covalency in the metal–ligand bonding of the cationic cobalt complexes consistent with large substituent shifts of the electrochemical reduction potentials and large NMR contact shifts of protons at the ligand rings and ligand methyl groups. Whether this trend is associated principally with an increase in the positive charge (cf. 4^+ vs. 1^{2+} and **2** vs. 3^+) of the complex or with the greater asymmetry of the mixed as opposed to symmetrical sandwich systems is the subject of further studies on unsymmetrical d^7 sandwich complexes presently under way in our laboratories.

Acknowledgment. Support from the Deutsche Forschungsgemeinschaft and the Swiss National Science Foundation is gratefully acknowledged. We are indebted to Dr. H. Lueken, Institute of Inorganic Chemistry, Technical University Aachen, for the susceptibility measurements of $3gPF_6$.

Registry No. 1(PF₆)₂, 69027-58-3; 1PF₆, 53382-65-3; 1^{2+} , 53382-67-5; **1b**, 68868-86-0; $1b^{2+}$, 51509-88-7; $1b^+$, 37298-45-6; **2a**, 51812-05-6; $2a^+$, 51364-24-0; **2gPF₆**, 71713-57-0; **3a**(PF₆)₂, 89031-67-4; **3aPF₆**, 90246-07-4; **3a**, 90246-08-5; $3a^{2+}$, 72339-93-6; $3a^+$, 90246-06-3; **3a**(BF₄)₂, 72339-94-7; **3b**(PF₆)₂, 90245-91-3; **3bPF₆**, 90246-05-2; **3c**(PF₆)₂, 90245-92-4; **3cPF₆**, 90246-03-0; **3d**(PF₆)₂, 90245-93-5; **3dPF₆**, 90246-01-8; **3e**(PF₆)₂, 90245-95-7; **3ePF₆**, 90245-99-1; **3f**(PF₆)₂, 79826-60-1; **3fPF₆**, 90245-97-9; **3fCl₂**, 90246-10-9; **3g**(PF₆)₂, 79826-62-3; **3gPF₆**, 90246-12-1; $3g^+$, 79826-61-2; **4**(PF₆)₂, 53382-63-1; [Co(pmcp)Cl₂]₂, 82595-77-5; [Co(pmcp)Br₂]₂, 82595-78-6; [Co(pmcp)Cl]₂, 74353-89-2; [Co(pmcp)Br]₂, 90246-09-6; Co(cp)₂, 1277-43-6; AlCl₃, 7446-70-0; Na₂S₂O₄, 7775-14-6.

(52) c_{π}^2 is given as 0.87 for Fe(cp)(bz) and 0.83 for Fe(hmbz)₂¹⁹ and 0.66 for Co(cp)₂ in Ru(cp)₂.²⁵